Numerical analysis of three dimensional flow around marine propellers in restricted water

2013 IOP Conf. Ser.: Mater. Sci. Eng. 50 012046

(http://iopscience.iop.org/1757-899X/50/1/012046)

Numerical analysis of three dimensional flow around marine propellers in restricted water

M Nakisa, A Maimun[a], Y M Ahmed and F Behrouzi
Mechanical Eng. Faculty, Universiti Teknologi Malaysia (UTM), 31810, Johor Bahru, Malaysia

[a]E-mail: adi@fkm.utm.my

Abstract. Marine propeller blades have complicated geometries and as a consequence, the flow pattern around these propellers is very complex. The efficiency of the marine propeller is strongly dependent on propeller performance, thrust force and torque of propeller. In channels, canals, harbors and other types of restricted waters, flow inlet to the propellers is asymmetric and non-uniform, therefore hydrodynamic characteristics of the propeller is affected greatly by the presence of lateral restrictions of the navigation area, such as banks, quay walls and bottom. This research has approached the propeller hydrodynamic performance related to study on wake pattern behind of propeller affected by bank via numerical modeling using a finite volume code. Finally, the results of simulation the propeller's wake pattern and 3D flow around the propeller, with and without bank are compared. The influence of these parameter changings in the working propeller performance are carefully considered and analyzed.

1. Introduction

Nowadays, with increasing the main particular size of certain ships such as LNG vessels, oil tankers and container ships, ship navigators are considered to navigate in confined waters such as channels and ports, because the access channel dimensions are not increased at the same rate. Moreover, the restricted vertically and laterally in waterways are affected on ship maneuvering and behavior [1-3]. It is well known that when a ship travels along a bank, the asymmetric flow around the ship induced by the bank causes a pressure difference between the port and starboard sides of the hull. As a result, a lateral force directed towards the bank and a yaw moment pushing away the bow will act on the ship. The fact is the so-called bank effects. Bank effects have a significant impact on the navigation safety when a ship sails along a bank. If the distance between ship and bank is very small, ship-bank collision may happen. When the water becomes shallow, the hydrodynamic forces induced by bank effects will change greatly. The sway force acting on a ship moving along a bank in an extremely shallow water way may be towards or away from the bank [3-8]. So, the study of bank effects for a ship sailing in shallow channel is very important to ensure the navigation safety. [9] found that the hydrodynamic coefficients were severely affected by the presence of lateral banks. He investigated the bank effects on ship manoeuvring behavior by varying the hull form, water depth, ship speed, ship-bank distance, bank slope and propeller rotation rate. They found that the direction and magnitude of the bank-

induced sway force and yaw moment were dependent on the above-mentioned parameters when water depth to draught ratio is less than 1.5.

With the fast development of the computer technology in recent decades, great progresses have been made in application of computational fluid dynamics (CFD)-based numerical methods to predict ship manoeuvring hydrodynamic forces. Some numerical methods were developed and applied to study the bank effects. Yasukawa developed a method by combining the slender body theory with panel method to calculate the lateral force and yaw moment acting on a ship in the proximity of arbitrary shaped bank [10-11]. [12] calculated sway force and yaw moment acting on a ship traveling off the centerline of a rectangular channel by using a numerical approach based on Dawson's method. [13] performed a series of numerical simulations to analyse the bank effects for a container ship in restricted waters by using commercial CFD software.

In this paper, in the numerical study, a LNG carrier' propeller sailing along the bank in a shallow channel is taken as example. A vertical bank and shallow water are considered. The influence of restricted water on thrust force, torque and efficiency of the propeller are calculated and analysed. The numerical results are compared with the available open water simulation that verified by experimental results.

2. Propeller Model

In this study one propeller in model scale, which is extensively used for the validation of CFD code in open water, is considered then, in according to this modeling the bank effect on propeller performance is considered. The propeller has a diameter D of 7.7 m and hub diameter D_{hub} of 0.17D, and is right handed when mounted on a pulling thrust. Design pitch ratio (P/D) is 0.94 and the blade ratio subjected to expanded area ratio (EAR) is 0.88. It's rake degree is 15degrees as well.

A propeller geometric characteristics and drawing are depicted in table 1 and figure 1, respectively.

Table 1. Propeller geometric characteristics

Parameter	Dimension
Z	5
D	7.7 m
D_{hub}	1.28 m
Br	0.17
P/D	0.94
A_e/A_0	0.88
R	15 Deg.

Figure 1 shows the propeller's front view which is can see in behind of ships and calculate the thrust and torque results of the kinetic energy of flow motion as well. That means propellers generate thrust through the production of lift by their rotating blades. This considered propeller is rotating right hand for making the axial force by push the water.

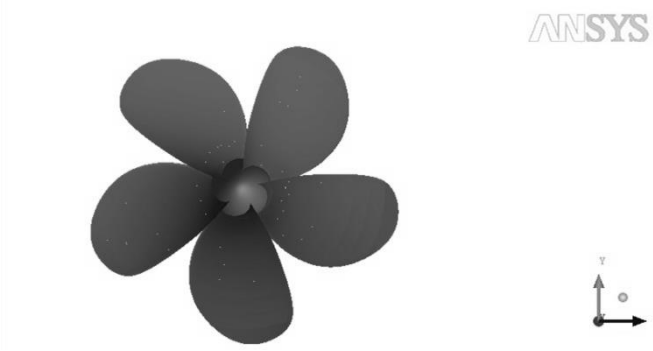

Figure 1. Front view of propeller

3. Boundary Condition

The numerical predictions presented in this work were carried out with the ANSYS-FLUENT 13, commercial CFD solver. It employs the node centred finite volume method. Figure 2(a), 2(b) and table 2 show the schemes and dimensions of computational domain for modelling and simulation of the propeller with and without bank, respectively. Table 2 shows the rotational and stationary computational domain dimensions respect to propeller diameter. The stationary domain dimension should be far from rotational domain to decrease the effect of wall side effects on the results.

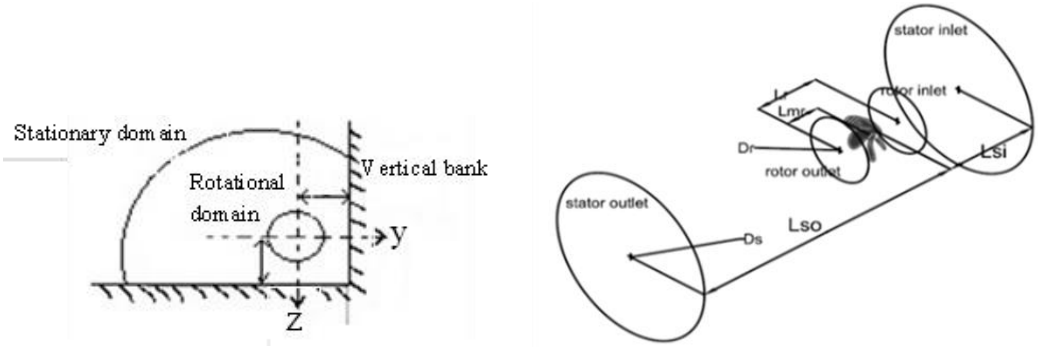

(a) Open water condition **(b)** Restricted water conditions

Figure 2. Schemes of computational domain

Table 2. Dimensions of computational domain (Based on Propeller diameter)

Value	Rotational	Stationary
D_r	1.44 D	
L_{mr}	1.5 D	
L_r	3 D	
D_s		10 D
L_{si}		3 D
L_{so}		5 D
d		1.7 D

In to a rotating part, called Rotating domain and in to a stationary part, called Stationary domain. The dimensions of the domains of propeller are given in table 2 that the variable L_{mr}, visible in figure 2 is the axial length of outlet the Rotating part, D is the propeller diameter and d is the distance between bank and centre of shaft. The inlet, outlet and outer boundaries of the Stationary part were placed far enough from the propeller in order to not affect the results. The distances were set through a domain independence study, carried out considering more shapes of the Stationary part, defined varying systematically L_r, L_{si}, D_s that shows in figure 3(a) and 3(b). Table 3 is shown the mesh information of domains with and without bank that are known as open water and restricted water.

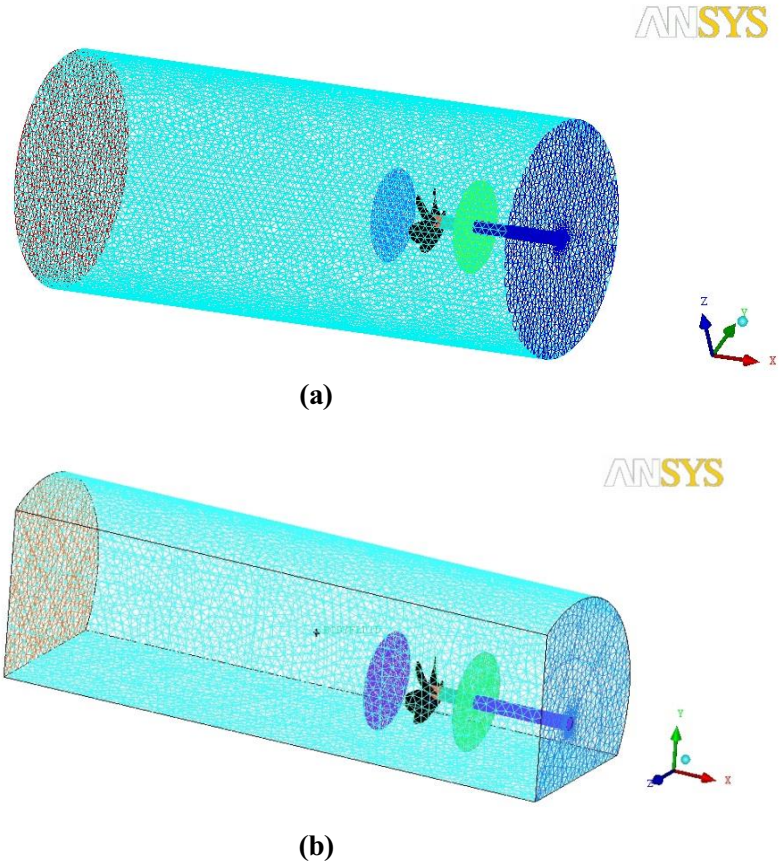

Figure 3. Rotational and Stationary domains for propeller working in (a) Open water and (b) Restricted water, generated using ICEM-CFD

Table 3. Mesh information of domains in open and confined water

Computational Domain	Total Elements	Total Nodes
Open water	393893	80634
Restricted water	171629	51389

4. Numerical Simulation

In Cartesian tensor form the general RANS equation for continuity can be written as:

RANS equation: $$\frac{\partial \rho}{\partial t} + \frac{\partial (\rho u_i)}{\partial x_i} = 0 \quad (1)$$

The equations for momentum become:

$$\frac{\partial (\rho u_i)}{\partial t} + \frac{\partial (\rho u_i u_j)}{\partial x_j} = \quad (2)$$

$$-\frac{\partial p}{\partial x_i} + \frac{\partial}{\partial x_j}\left[\mu\left(\frac{\partial u_i}{\partial x_j} + \frac{\partial u_j}{\partial x_i} - \frac{2}{3}\delta_{ij}\frac{\partial u_i}{\partial x_i}\right)\right] + \frac{\partial}{\partial x_j}(-\rho\overline{u_\iota' u_j'})$$

Where δ_{ij} is the Kronecker delta, $(-\rho\overline{u_\iota' u_j'})$ are the unknown Reynolds stresses that have to be modeled to close the momentum equation. With Boussinesq's eddy-viscosity assumption and two transport equations for solving a turbulence velocity and turbulence time scale (turbulence modeling), RANS equations are closed.

Only steady incompressible equations are solved in the present work. The shear-stress transport SST k-e model with the "transitional flow option" is employed here due to its good performance for wall-bounded boundary layer flows. The FLUENT 13 code is used to solve the three dimensional viscous incompressible flow. The parallel version of FLUENT simultaneously computes the flow equations using multiple processors. The software can automatically-partitions the grid into sub-domains, to distribute the computational job between available numbers of processors.

Simulations in this paper are completed using FLUENT software, SST (k-w) model and standard wall function. Some major parameters are set as shown in table 4 while the other options remain default. Force and momentum data are recorded every step.

Table 4. Computational setting

Parameter	**Setting**
Computing	64-bit Desktop pc 6GB of RAM
Simulation type	Steady state
Mesh type	Unstructured hybrid(tetrahedral/prism)
Turbulence model	k-w (Shear stress transport)
Wall modeling	Automatic wall function based on a law of the wall formulation
Advection scheme	CFX high resolution

The shear-stress transport SST (k-w) model is used for turbulence closure in this research. The SST (k-w) model is an empirical model transport equations solving for the turbulence kinetic energy (k) and the specific dissipation rate (w) and remained as one of the most accurate and reliable turbulence models for external hydrodynamics.

κ function: $$\frac{\partial}{\partial t}(\rho k) + \frac{\partial}{\partial x_i}(\rho k u_i) = \frac{\partial}{\partial x_j}\left(\Gamma_k \frac{\partial k}{\partial x_j}\right) + G_k - Y_k + S_k \quad (3)$$

ω function: $$\frac{\partial}{\partial t}(\rho \omega) + \frac{\partial}{\partial x_i}(\rho \omega u_i) = \frac{\partial}{\partial x_j}\left(\Gamma_\omega \frac{\partial \omega}{\partial x_j}\right) + G_\omega - Y_\omega + D_\omega + S_\omega \quad (4)$$

Where G_κ and $G_\omega$represents the generation of turbulence kinetic energy due to mean velocity gradients and the generation of ω. Γ_κ and $\Gamma_\omega$represent the effective diffusivity of κ and ω. Y_κ and Y_ω represent the dissipation of κ and ω due to turbulence. D_ω represents the cross-diffusion term, S_κ and S_ω are user-defined source terms [13].

5. Results and Discussion

Pressure distribution on the surface of blade is shown in figure 4 that the face and back are experiencing high pressure and low pressure respectively. This explains the development of thrust by propeller at high pressures whereas the propeller is contributing to resistance and friction coefficient that shows in figure 5(a) and 5(b). It is evident that there is a concentration of high-pressure region near the leading edge of the propeller.

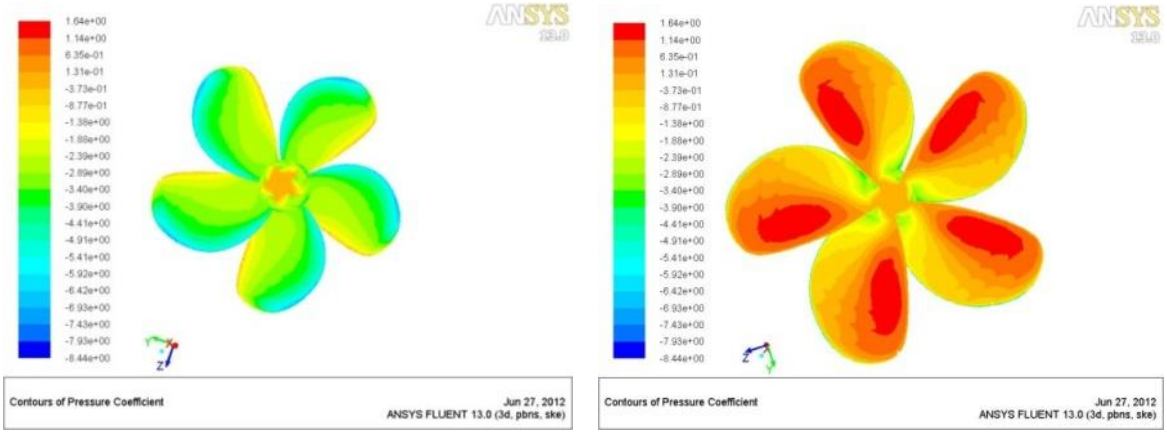

(a) Back side of the propeller (b) Face side of the propeller

Figure 4. Propeller's blades pressure distributions

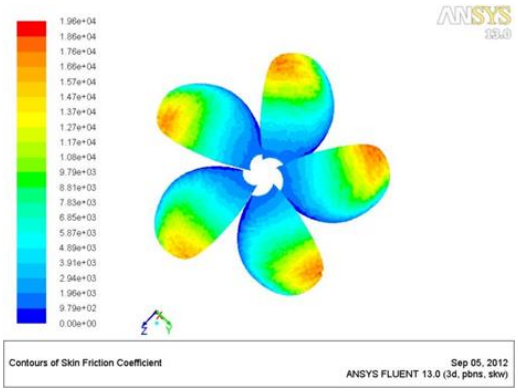

Figure 5. Contours of skin friction coefficient

Figure 6(a) and 6(b) show the distribution of pressure coefficient on face and back surface of one blade at three radial section r/R = 0.80. It is clearly that the low pressure region is happen on back surface and the high pressure region is occurred on face surface of blade. Figure 7(a) and 7(b) show

the contours and velocity distribution on face of blades that the high velocity is occurred near the tips of blades.

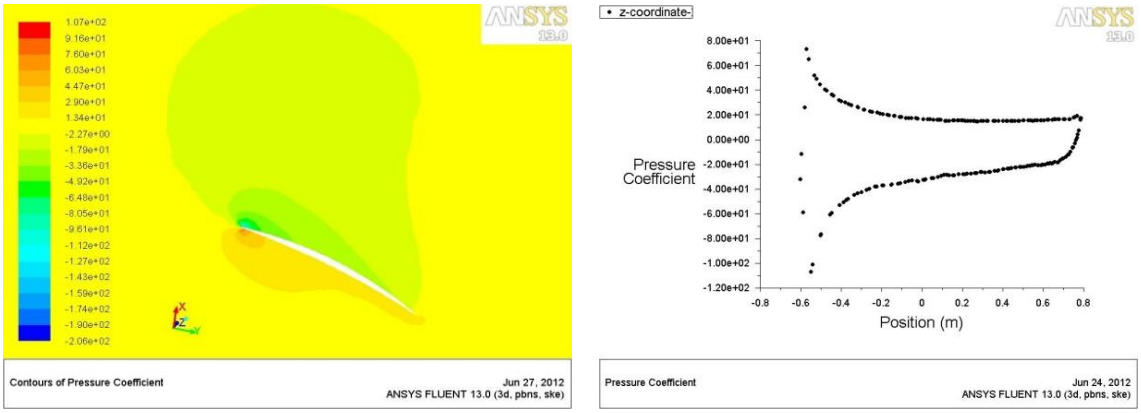

(a) Pressure distribution contours (b) Pressure coefficient

Figure 6. Pressure coefficient on blade section

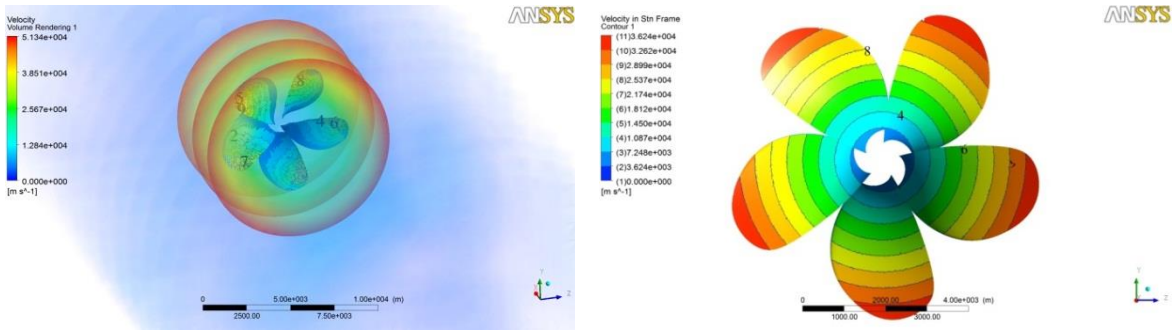

(a) (b)

Figure 7. Velocity magnitudes around the propeller blades in (a) and (b) views

When a ship sails on a canal or other restricted waterway the propeller of ship will experience a higher velocity inlet than sailing in open water. The effects of bank and shallow water on the longitudinal force and momentum are taken into account by the thrust and torque coefficient. As a consequence the influence of the bank and shallow water are not calculated independently.

A ship sailing within the horizontal reach of a bank will be attracted to the closest bank when the under keel clearance exceeds a minimum value. In according to velocity vectors and contours in restricted water in comparison with open water condition that are shown in figure 8(a), 8(b), 9(a) and 9(b), While she sails in shallow water the propeller will be pushed the stern of ship near the bottom because the outlet vectors go up than in open water.

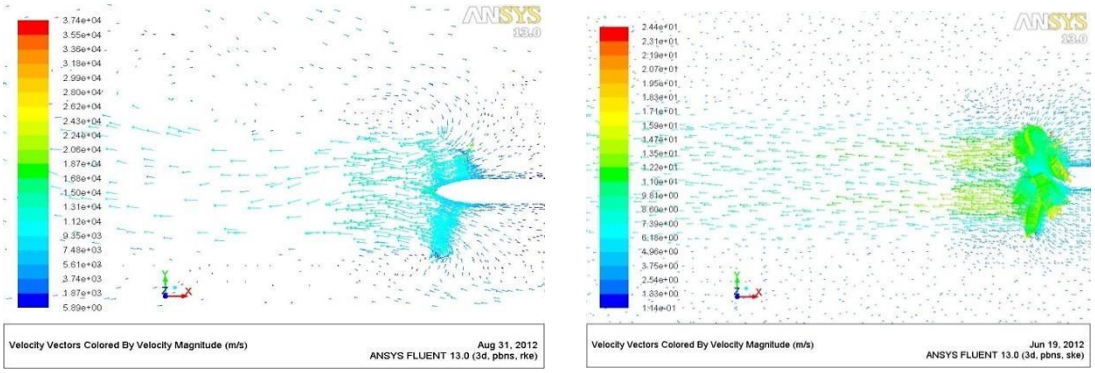

(a) Shallow water condition (b) open water condition

Figure 8. Velocity vectors behind the propeller

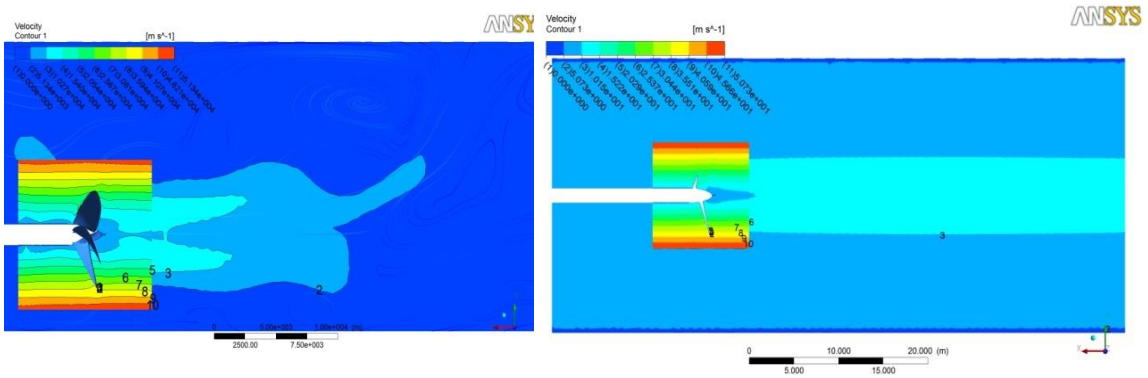

(a) Shallow water (b) Open water

Figure 9. Velocity contours behind the propeller with and without bank

The forces and moments produced by the propeller are expressed in their most fundamental form in terms of a series of non-dimensional characteristics: these are completely general for a specific geometric configuration. The non-dimensional terms used to express the general performance characteristics are as follows:

Thrust coefficient: $$K_t = \frac{T}{\rho n^2 D^4} \quad (5)$$

Torque coefficient: $$K_Q = \frac{Q}{\rho n^2 D^5} \quad (6)$$

Advance coefficient: $$J = \frac{V_a}{nD} \quad (7)$$

The results from the Numerical simulation of propeller in open and restricted water based on RANS equation at full scale compared to the model test results can be seen in figure 9 Various J-values are obtained by keeping a same revolutions (n=90 rpm) but varying the flow speed. The trends of results with varying advance ratio are well predicted. It should be noted that K_Q and K_t are slightly

over predicted all the way. The maximum hydrodynamic propeller efficiency will be occurred in j=0.84 and j=0.87 for open water and restricted water, respectively.

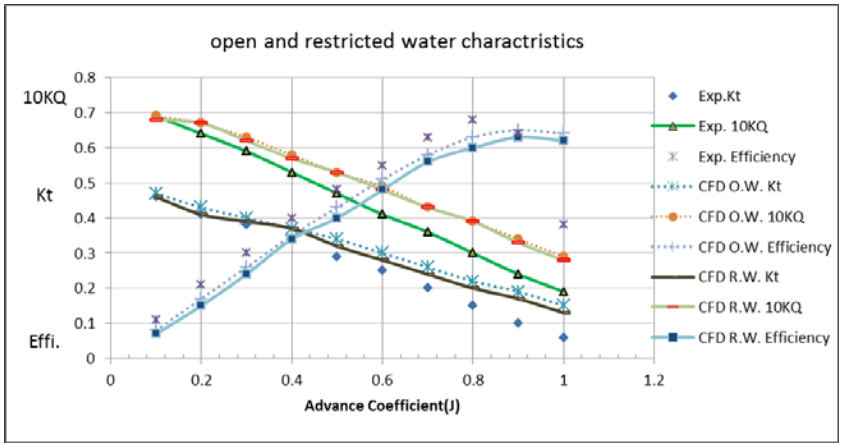

Figure 10. Open and restricted water diagram of propeller performance at full scale

6. Conclusion

In according to the presented computational results based on RANS equations, the following conclusions are taken:

- The hydrodynamic propeller performance is influenced by the proximity of bank and shallow water.
- The forces and moments acting on the propeller when operating in a uniform fluid stream, hence the propeller generate the thrust and make pressure and velocity in the fluid particles on face blades surface and behind the propeller.
- The fluid velocity in the tips of blades is higher than other areas and the pressure distribution in the face blades near leading edges is higher than other areas.
- The maximum hydrodynamic propeller efficiency will be occurred in j=0.84 and j=0.87 for open water and restricted water, respectively

Acknowledgements

The authors would like to thank the Faculty of Mechanical Engineering in Universiti Teknologi Malaysia (UTM) for financial support under MOHE-UTM-Vote No. 00G44.

References

[1] Ch'ng P W, Doctors L J, Renilson M R 1993 A method of calculating the ship-bank interaction forces and moments in restricted water *International Shipbuilding Progress* **40**(421) 7-23.
[2] Li Da-qing, Ottosson P, Tr¨agardh P, 2003 Prediction of bank effects by model tests and mathematical models [C]/ *Proceedings MARSIM'03, International Conference on Marine Simulation and Ship Maneuverability*. Kanazawa, Japan: [s.n.], RC**30**.1-12.
[3] Tahseen T A, Ishak M and Rahman M M 2012 *J. Mech. Eng. Sci.* **3** 271.
[4] Tahseen T A, Ishak M and Rahman M M 2013 *J. Mech. Eng. Sc.* **4** 418.
[5] Al- Doori, W H A R 2011 *Inter. J. Automot. Mech. Eng.* **4** 428.
[6] Tahseen T A, Ishak M and Rahman M M 2012 *Inter. J. Automot. Mech. Eng.* **6** 753.
[7] Ishak, M., Tahseen, T A and Rahman, M M 2013. *Inter. J. Automot. Mech. Eng.* **7** 900.

[8] Vantorre M, Delefortrie G, Eloot K, et al. 2003 Experimental investigation of ship-bank interaction forces *Proceedings MARSIM'03, International Conference on Marine Simulation and Ship Maneuverability*. Kanazawa, Japan, RC**31**.1-9.
[9] Norrbin N H 1974 Bank effect on a ship moving through a short dredged channel [C]// *Proceedings 10th Symposium on Naval Hydrodynamics*. Cambridge, MA, USA 71-87.
[10] Yasukawa H 1991 Bank effect on ship maneuverability in a channel with varying width [J]. *Transactions of the West-Japan Society of Naval Architects*, **81**: 85-100.
[11] Miao Quang-ming, Xia Jin-zhu, Chwang A T, et al. 2003 Numerical study of bank effects on a ship traveling in a channel [C]/*Proceedings 8th International Conference on Numerical Ship Hydrodynamics*. Busan, Korea 266-273.
[12] LoDC, Su Dong-taur, Chen Jan-ming 2009 Application of computational fluid dynamics simulations to the analysis of bank effects in restricted waters *The Journal of Navigation*, **62** 477-491.
[13] Maimun, A, Yasser M Ahmed., Priyanto A, Y S Ang., M Nakisa 2012 Assessment of Ship-Bank Interactions on LNG Tanker in Shallow Water, University Technology Malaysia, Johor Bahru, Malaysia, *Proceeding of 6th Asia-Pacific Workshop on Marine Hydrodymics-APHydro12 Malaysia*, September 3-4.

Nomenclature

D: Propeller diameter, (m)
Z: Number of blade
R: Rake of Blades
C_p: Pressure coefficient
p_0: Reference pressure at infinity
J: Advance ratio
K_Q: Torque coefficient
A_E/A_0= Expanded Area Ratio (EAR)
η = Open water efficiency
L_r= Length of rotational domain
D_{hub}: Hub diameter, (m)
P/D: Pitch Ratio
n: Rate of revolutions of propeller, (rpm)
p: Static pressure at point of interest
V_a: Advance velocity, (m/s)
K_T: Thrust coefficient
B_r: Boss ratio
ρ = Density of water
D_r= Diameter of Rotational domain